LECTURE 7.2

Josephson effect
and
Slow light

dr Barbara Piętka
barbara.pietka@fuw.edu.pl
pok. 3.64

Institute of Experimental Physics
Faculty of Physics
Warsaw University

Josephson effect

first described for superconductors

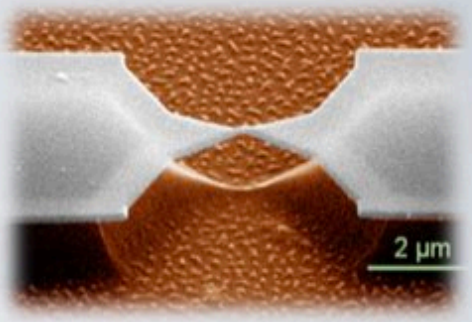

image source: CEA-SPEC, Saclay, France

B. J. Josephson in 1962:
oscillating current flow across two weakly coupled superconductors to preserve long-range order across the junction

➙ *any two macroscopic quantum systems separated by thin barrier*

MACROSCOPIC QUANTUM SYSTEMS

— superconductors
— bosonic condensates (atoms, photons, magnons, polaritons, ...)

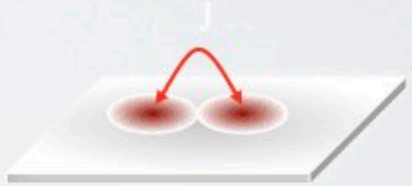

„Giant matter wave"

$$\psi = \sqrt{N} e^{i\theta}$$

— MASSIVE OCCUPATION OF GROUND STATE
— INCREASE OF TEMPORAL COHERENCE
— LONG RANGE SPATIAL COHERENCE

Josephson effect

main regimes

- *DC Josephson effect* (constant current)
  - small constant current applied resulting in a constant direct super-current flowing through barrier
  - no voltage drop across the junction

- *AC josephson effect* (alternating current)
  - upon constant chemical potential difference (voltage)
  - phase difference vary linearly in time
  - oscillating current across the junction

$$\frac{dN}{dt} : \sin(\Delta\theta)$$

$$\frac{d\Delta\theta}{dt} : const$$

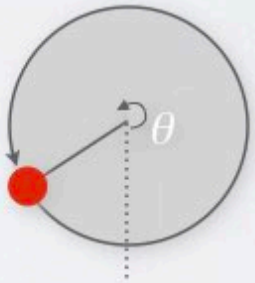

BOSONIC JOSEPHSON JUNCTION

bozonowe złącze Josephsona

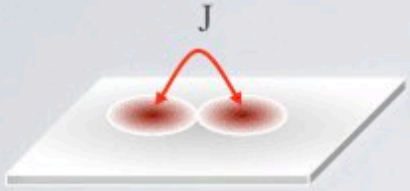

TWO SPATIALLY SEPARATED QUANTUM WELLS

WITH MACROSCOPIC POPULATION

- with E_1,N_1,θ_1 and E_2,N_2,θ_2
- Two parameters needed:

$$\Delta N = \frac{N_1 - N_2}{N_1 + N_2} \quad \text{and} \quad \Delta\theta = \theta_1 - \theta_2$$

ΔN - concentration difference

$\Delta\theta$ - phase difference

J - coupling constant

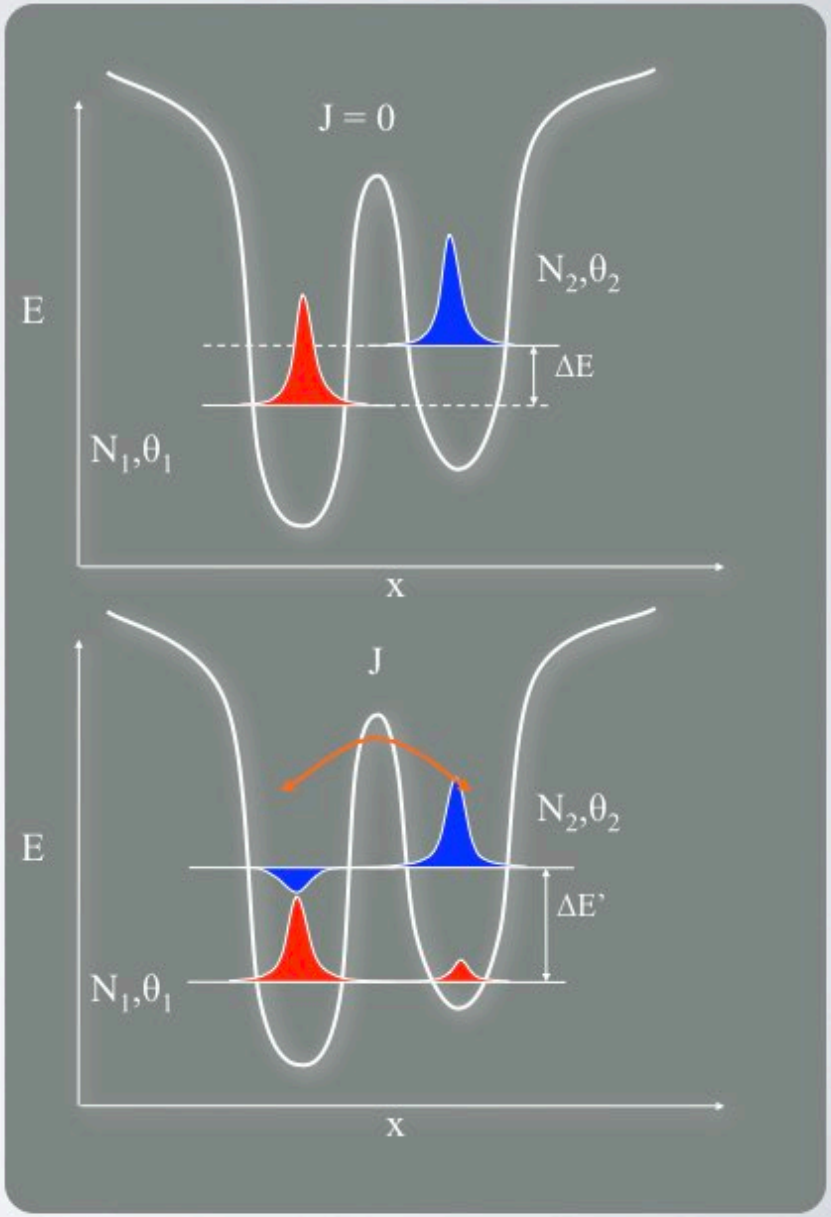

BOSONIC JOSEPHSON JUNCTION

bozonowe złącze Josephsona

System is described by coupled nonlinear Schrodinger equations

$$i\hbar\frac{\mathrm{d}\psi_{\mathrm{L}}}{\mathrm{d}t} = (E_{\mathrm{L}}^{0} + U|\psi_{\mathrm{L}}|^{2})\psi_{\mathrm{L}} - J\psi_{\mathrm{R}}$$

$$i\hbar\frac{\mathrm{d}\psi_{\mathrm{R}}}{\mathrm{d}t} = (E_{\mathrm{R}}^{0} + U|\psi_{\mathrm{R}}|^{2})\psi_{\mathrm{R}} - J\psi_{\mathrm{L}}$$

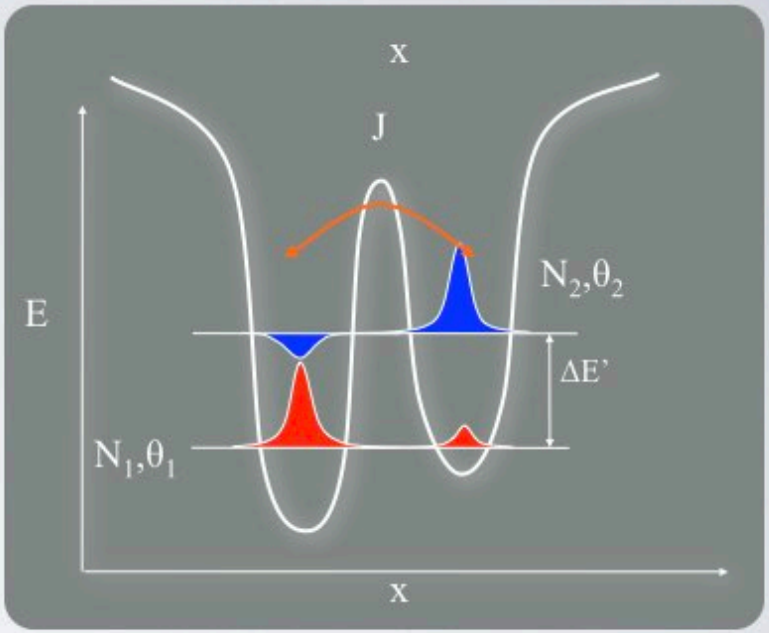

Using the transformation:

$$\psi_{\mathrm{L,R}}(t) = \sqrt{N_{\mathrm{L,R}}(t)}\,\mathrm{e}^{i\theta_{\mathrm{L,R}}(t)}$$

coupled equations take the form:

$$\frac{\hbar}{2J}\dot{z} = \sqrt{1-z^{2}(t)}\sin\phi(t)$$

$$-\frac{\hbar}{2J}\dot{\phi} = \frac{E_{\mathrm{L}}^{0} - E_{\mathrm{R}}^{0}}{2J} + \frac{UN_{\mathrm{T}}\mathrm{e}^{-t/\tau}}{2J}z(t) + \frac{z(t)}{\sqrt{1-z^{2}(t)}}\cos\phi(t)$$

where $z(t) = \frac{N_{\mathrm{L}}-N_{\mathrm{R}}}{N_{\mathrm{T}}}$ is the population imbalance

$N_{\mathrm{T}} = N_{\mathrm{L}} + N_{\mathrm{R}}$ the total population

$\phi(t) = \theta_{\mathrm{L}}(t) - \theta_{\mathrm{R}}(t)$ is the phase difference

BOSONIC JOSEPHSON JUNCTION - **ATOMIC GASES**

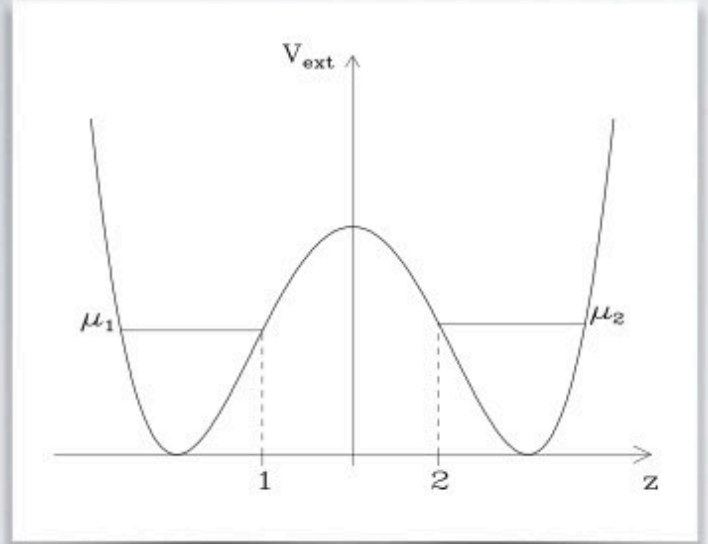

F. Dalfovo, Lp. P. Pitaevskii, S. Stringari, Rev. Mod. Phys. 71, 463 (1999)

$$\mu_1 \neq \mu_2 \quad (N_1 \neq N_2)$$

$$\theta_1 \neq \theta_2$$

$$I = I \sin \frac{(\mu_1 - \mu_2)t}{\hbar}$$

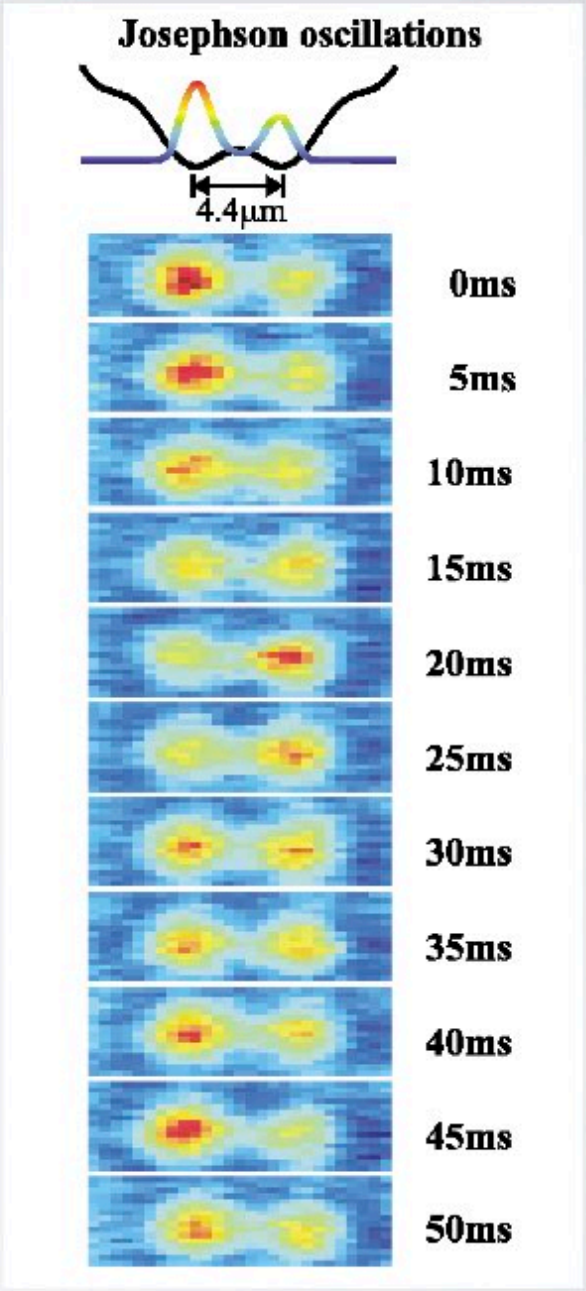

M. Albiez et al., PRL 95, 010402 (2005)

BOSONIC JOSEPHSON JUNCTION - ATOMIC GASES

Letter *Nature* **449**, 579-583 (2007)

The a.c. and d.c. Josephson effects in a Bose–Einstein condensate by S. Levy, E. Lahoud, I. Shomroni & J. Steinhauer

$$\dot{\eta} = \omega_J \sin\phi - G\Delta\mu$$

$$\eta \equiv (N_1 - N_2)/N$$

$$\Delta\mu = \hbar\omega_C\left(\eta - \eta_{equil}\right)$$

$$\dot{\phi} = -\frac{\Delta\mu}{\hbar}$$

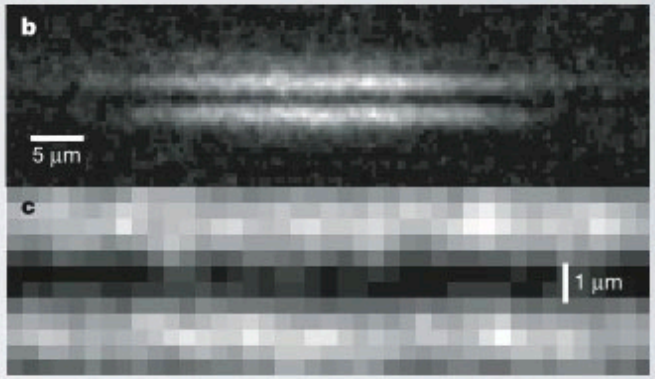

Creation of a BEC Josephson Junction

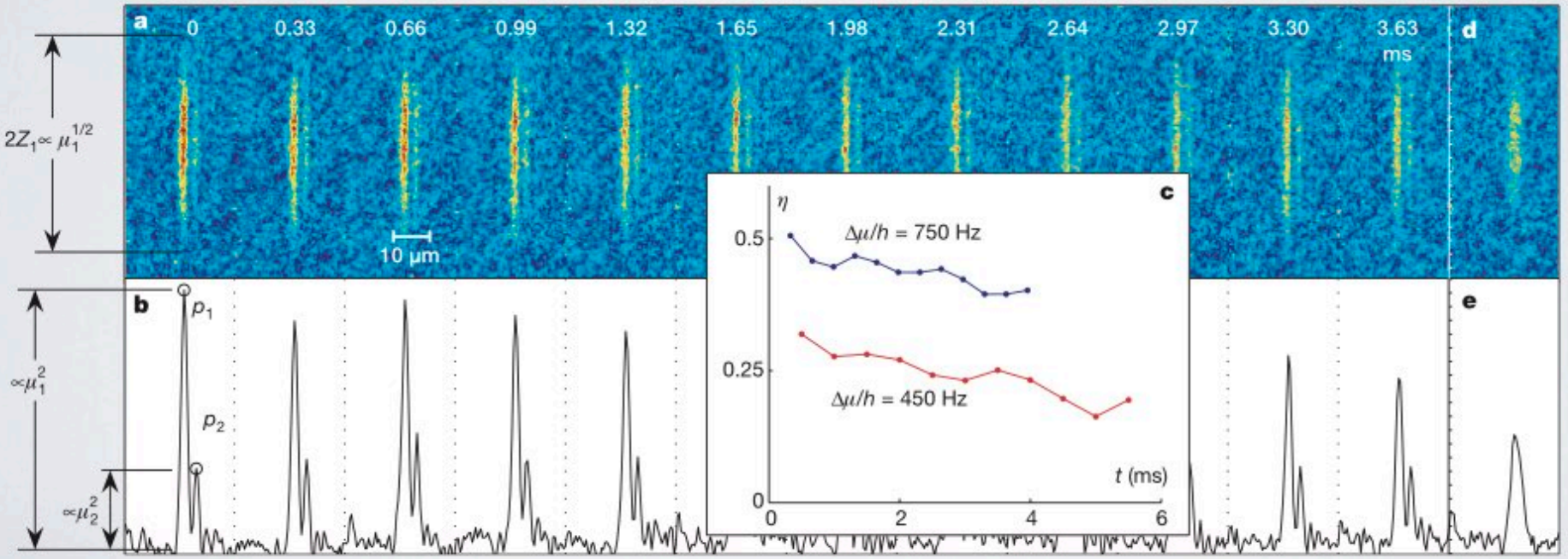

Time evolution of a BEC Josephson Junction

POLARITON CONDENSATE

NON-COHERENT GAS OF POLARITONS —*phase transition*→ CONDENSED STATE

polariton density ↗

non-equilibrium condensate seen in real space

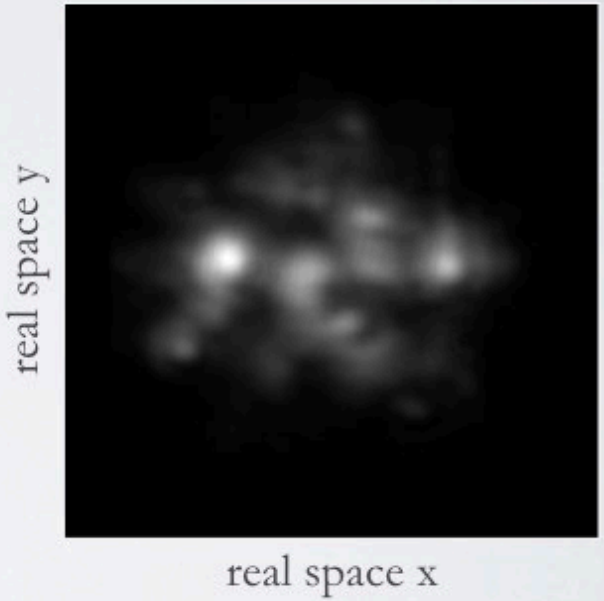

ADVANTAGES

- Disorder limited geometry

- Modification of wave function by the external parameter (lateral confinement)
- Control of the discrete states by an external laser

DISADVANTAGES

- Short lifetime & 10^6 of integrations
- Constant phase relation over many shots of the same experiment

EXCITON-POLARITON JOSEPHSON JUNCTION

TIME INTEGRATED REAL SPACE IMAGE

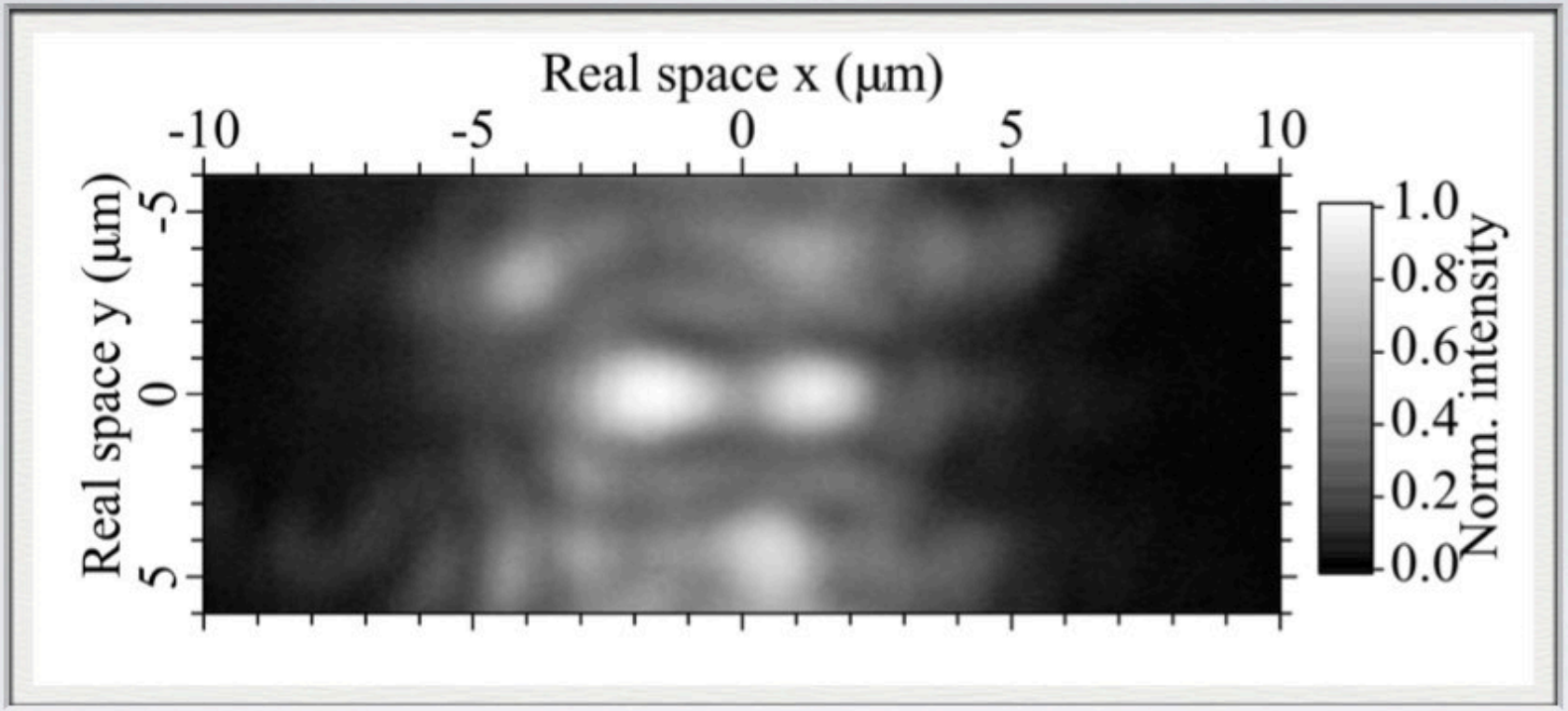

INTRINSIC DISORDER (PHOTONIC)

2μm SIZE TRAPS

DEPTH OF THE POTENTIAL : 5.6 meV

K. Lagoudakis et al., Phys. Rev. Lett. 105, 120403 (2010)

EXCITON-POLARITON JOSEPHSON JUNCTION

TIME INTEGRATED REAL SPACE IMAGE

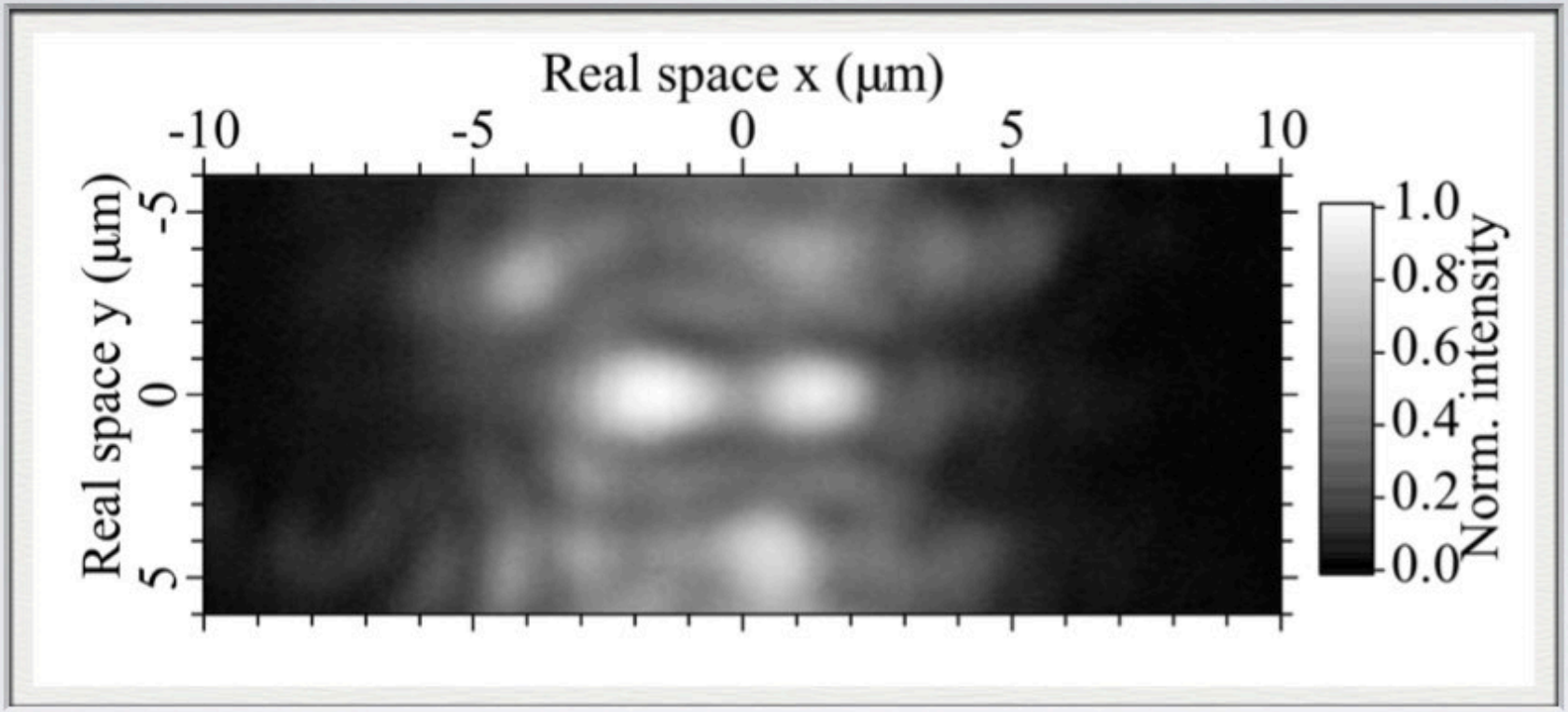

- To probe ΔN - temporally resolved real space imaging
- To probe $\Delta\theta$ - temporally resolved interference pattern of the two wells

K. Lagoudakis et al., Phys. Rev. Lett. 105, 120403 (2010)

EXPERIMENTAL METHODS

EXCITATION

- Pulsed Ti:Sapphire (250fs pulse duration; *f*=80MHz repetition rate)
- Non-resonant excitation (@695nm)

MICROSCOPE OBJECTIVE

- NA 0.5
- Spot size 15μm
- Diffraction limited resolution

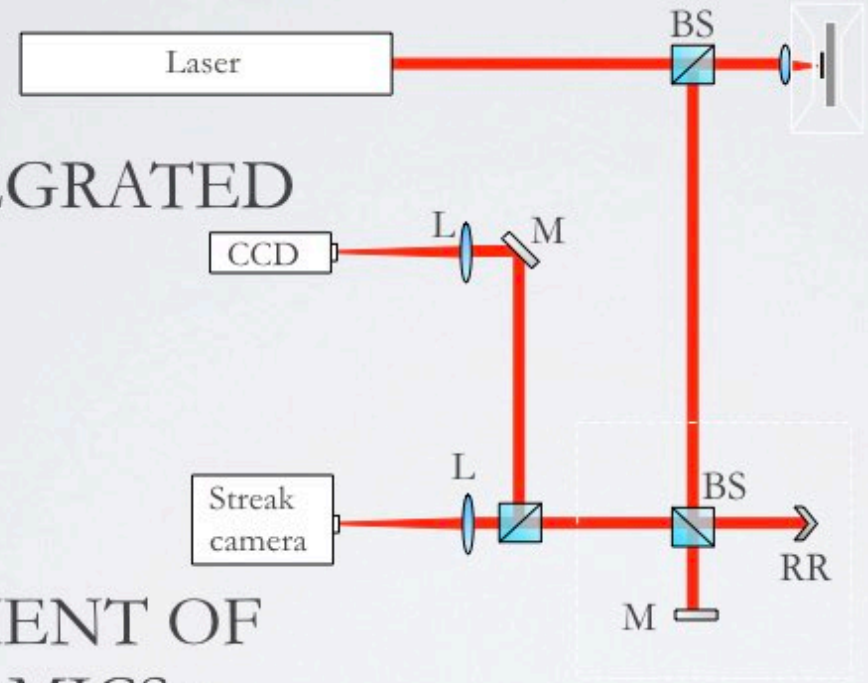

Sample on cold finger of cryostat

- Lattice temperature T = 10K

TIME INTEGRATED IMAGING :

Stabilized Michelson interferometer

MEASUREMENT OF TIME DYNAMICS :

- Time resolution limited to 3.5ps

POPULATION OSCILLATIONS IN POLARITON JOSEPHSON JUNCTION

POPULATION DYNAMICS

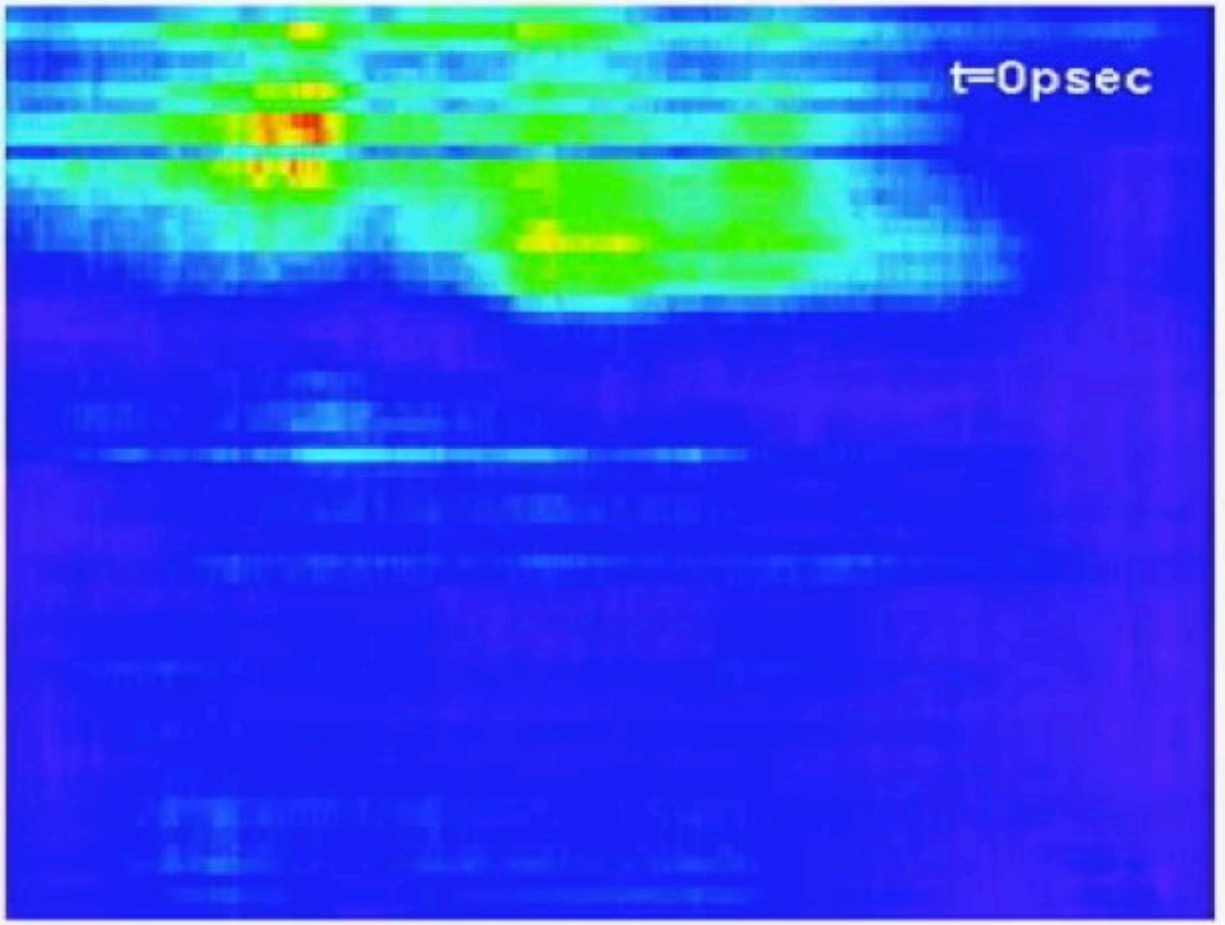

K. Lagoudakis et al., Phys. Rev. Lett. 105, 120403 (2010)

POLARITON JOSEPHSON JUNCTION

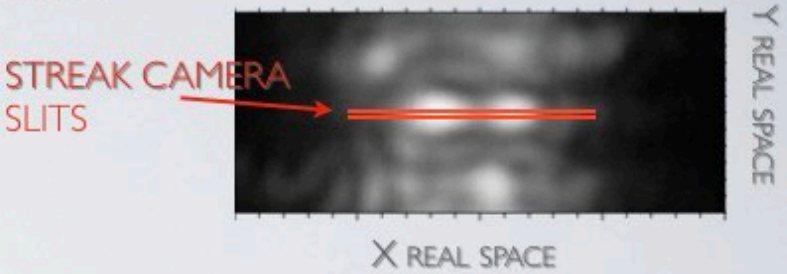

POPULATION DYNAMICS

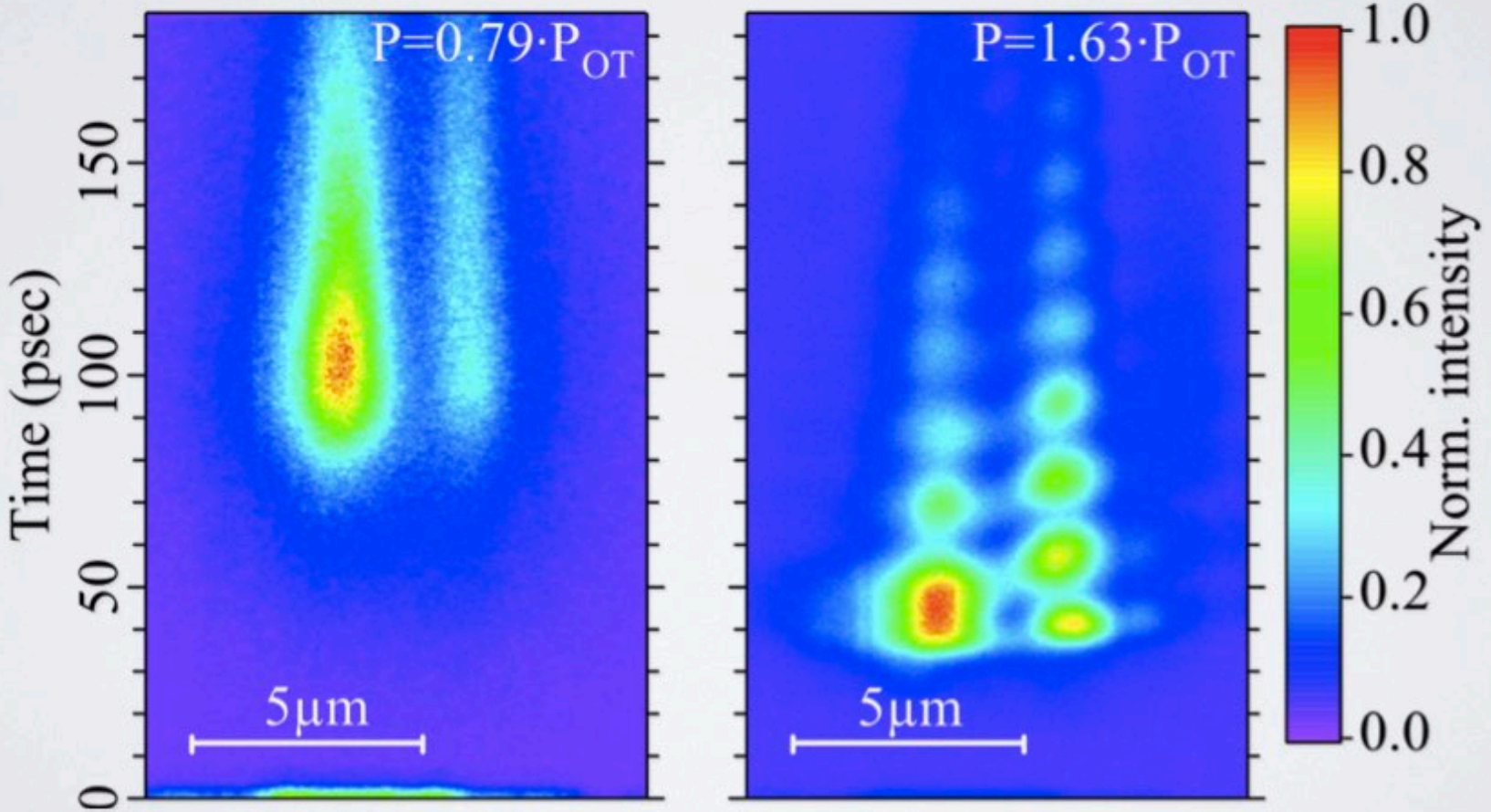

K. Lagoudakis et al., Phys. Rev. Lett. 105, 120403 (2010)

BELOW CONDENSATION THRESHOLD

ABOVE CONDENSATION THRESHOLD

POPULATION OSCILLATIONS IN POLARITON JOSEPHSON JUNCTION

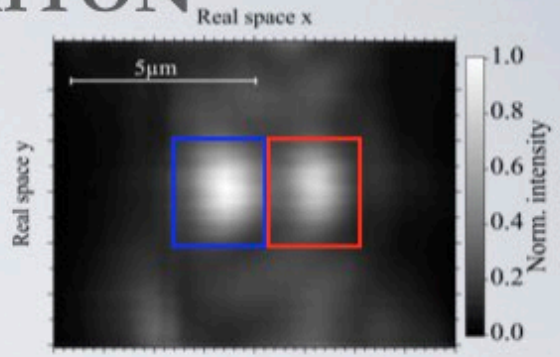

POPULATION PROFILES TAKEN ON EQUAL SIZE SQUARES

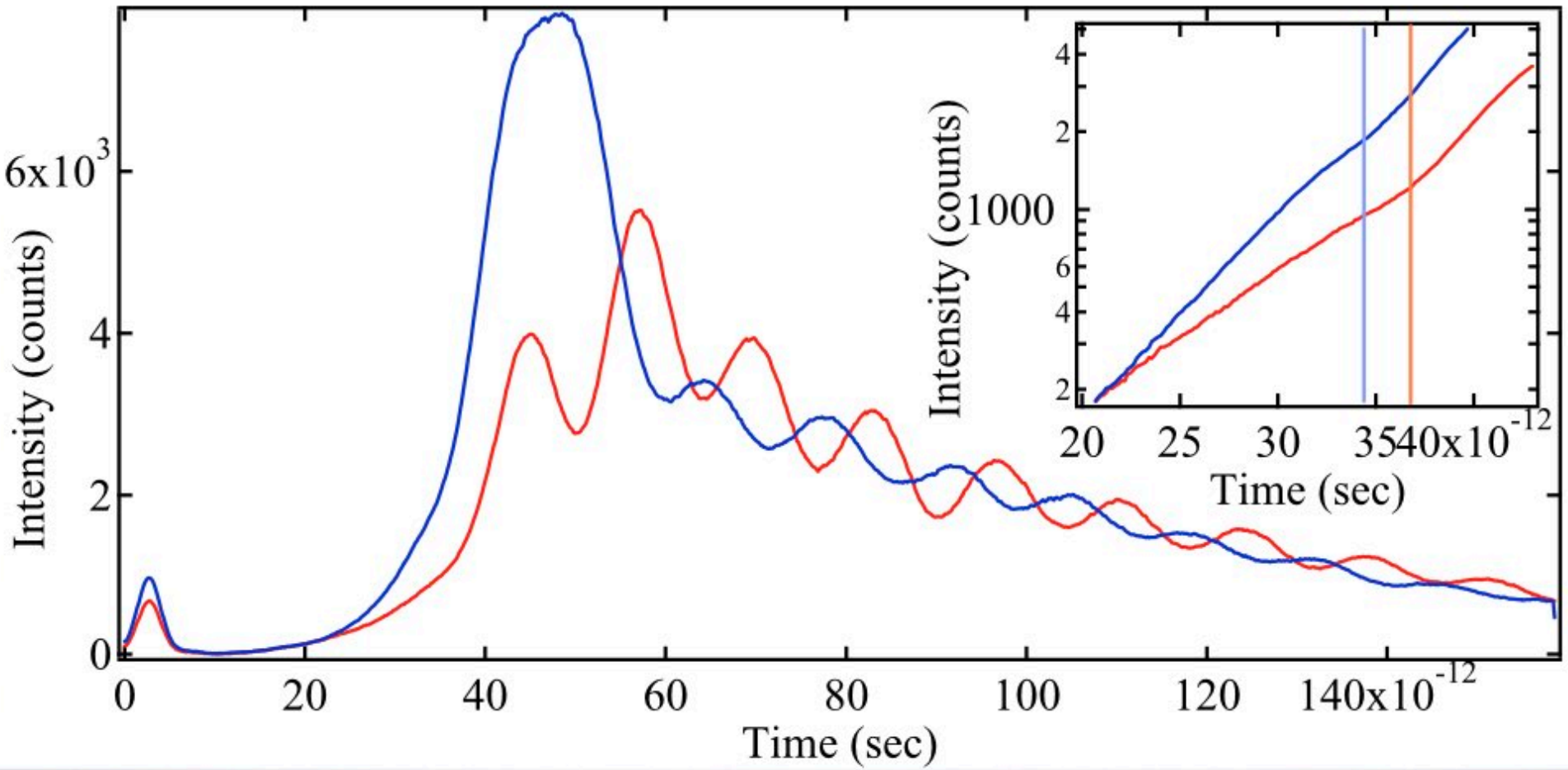

K. Lagoudakis et al., Phys. Rev. Lett. 105, 120403 (2010)

NORMALIZED POPULATION DYNAMICS

NORMALIZED POPULATION PROFILE

POPULATION DIFFERENCE

$$\Delta N = \frac{N_1 - N_2}{N_1 + N_2}$$

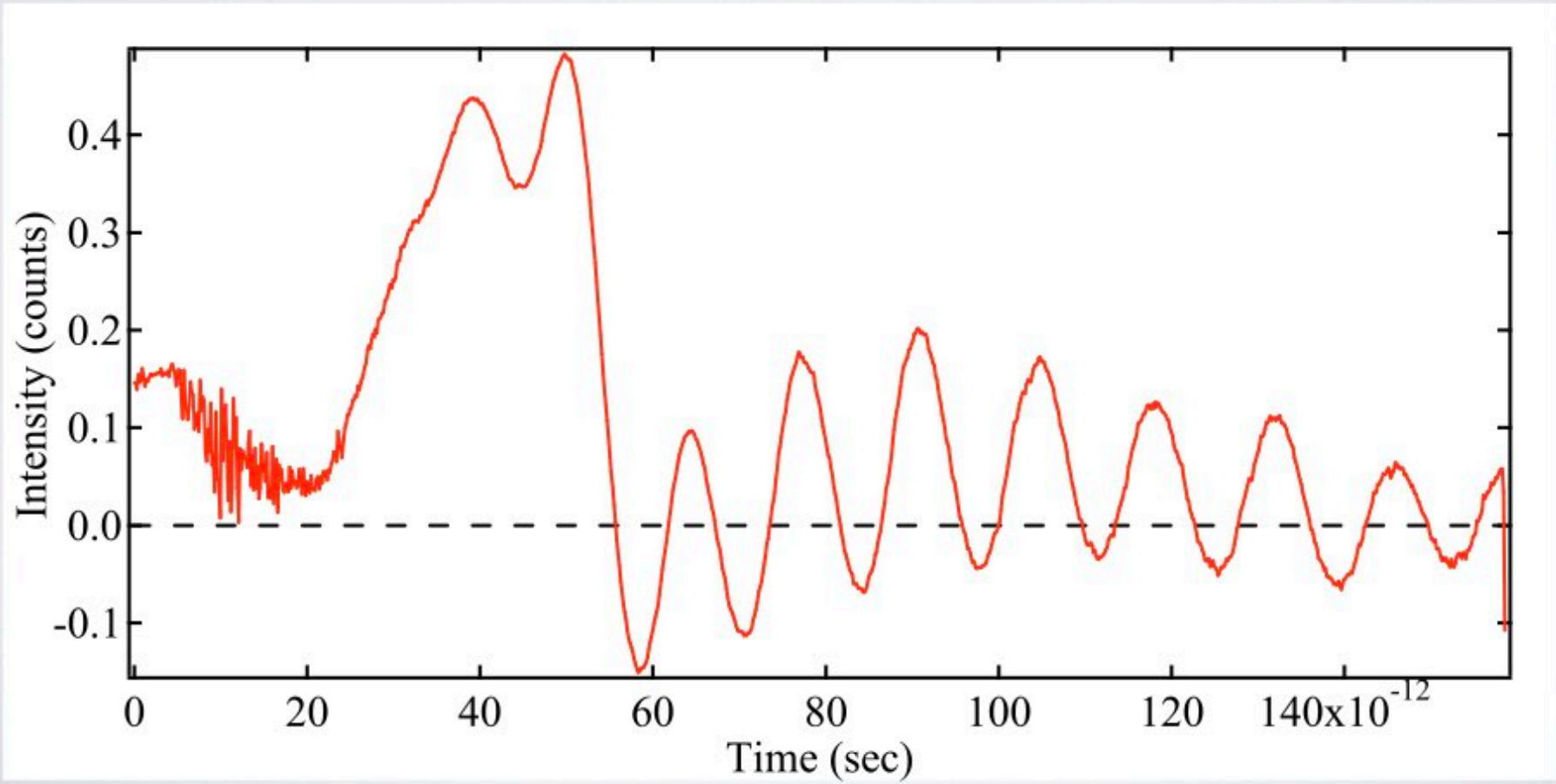

K. Lagoudakis et al., Phys. Rev. Lett. 105, 120403 (2010)

SPECTROSCOPIC STUDIES

FFT OF THE NORMALIZED POPULATION PROFILE :

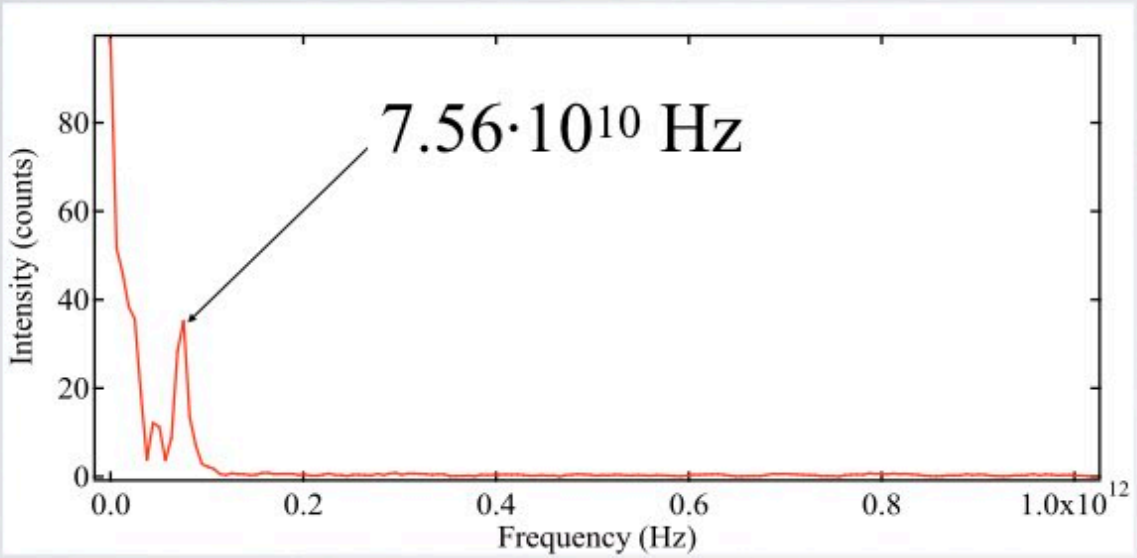

beating frequency corresponds to 312μeV

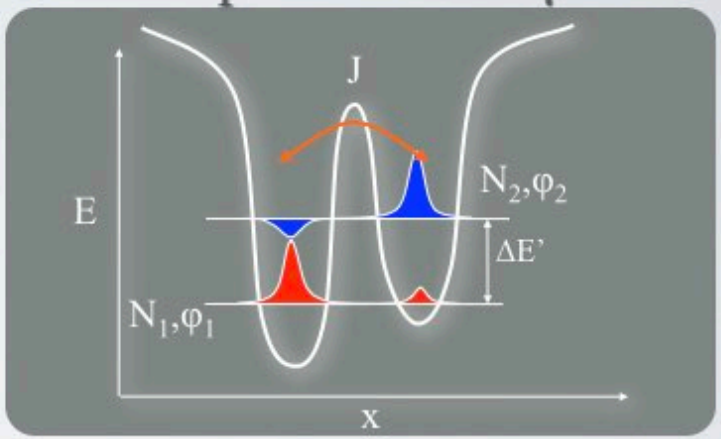

TIME INTEGRATED SPECTRUM UNDER PULSED EXCITATION :

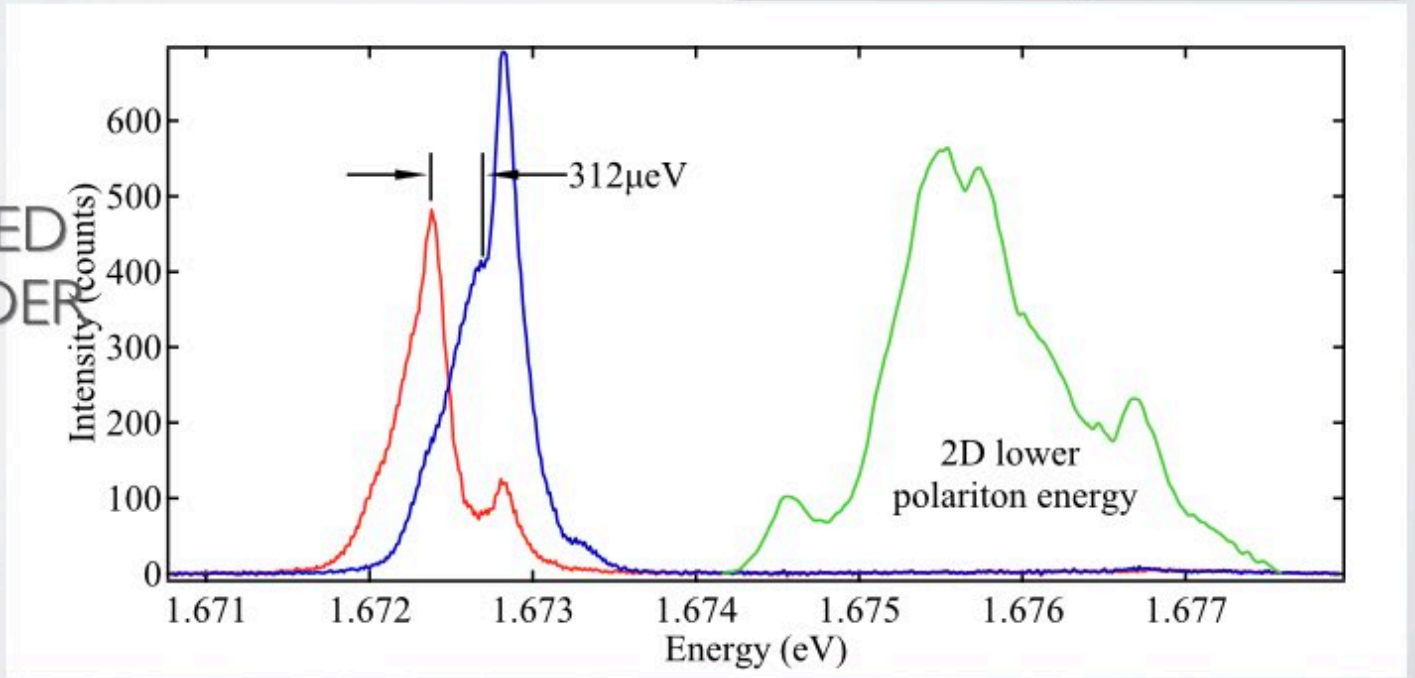

K. Lagoudakis et al., Phys. Rev. Lett. 105, 120403 (2010)

PHASE MEASUREMENT

PRINCIPLE

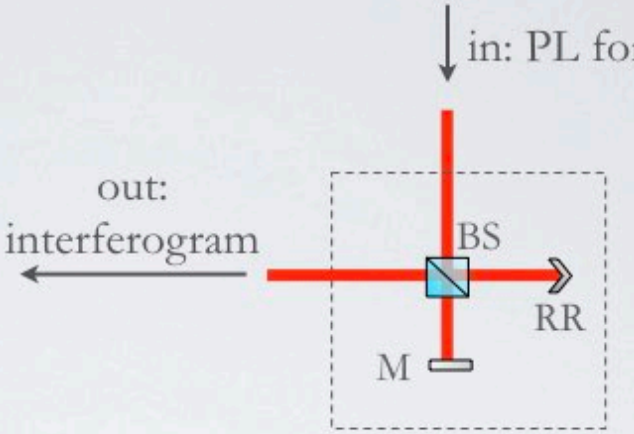

STREAK CAMERA
FOR TIME RESOLUTION

MICHELSON
INTERFEROMETER

EXPERIMENTAL REALIZATION

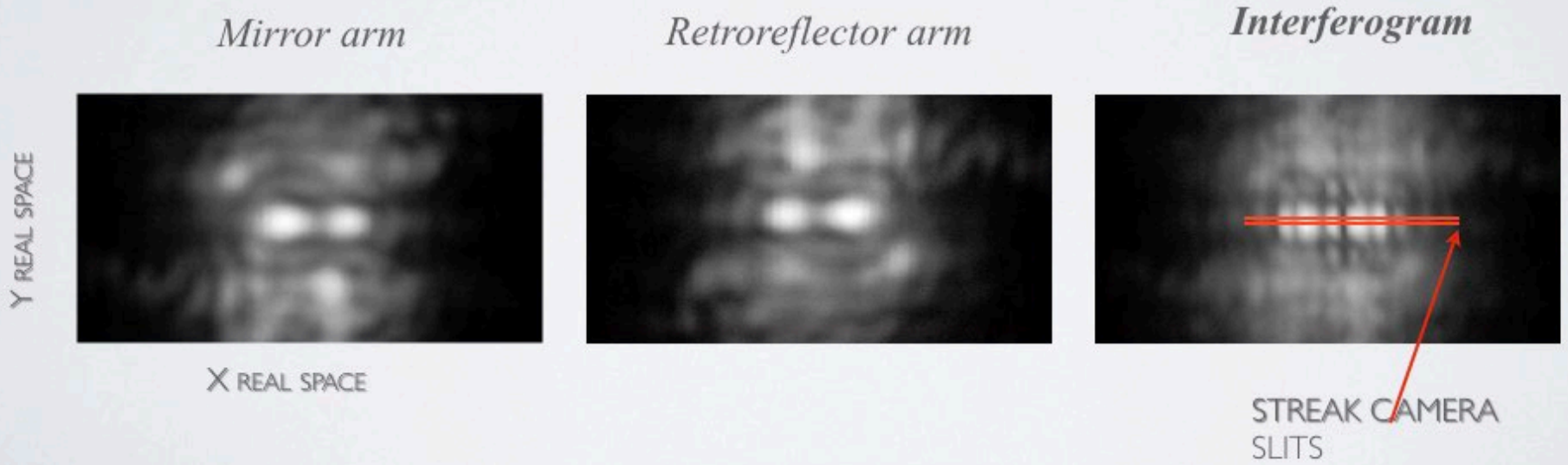

RELATIVE PHASE !!!

K. Lagoudakis et al., Phys. Rev. Lett. 105, 120403 (2010)

PHASE EVOLUTION IN TIME

- Sinusoidal vs linear phase evolution
- How it is expected in an interferometric measurement?

CONSTANT SINUSOIDAL LINEAR

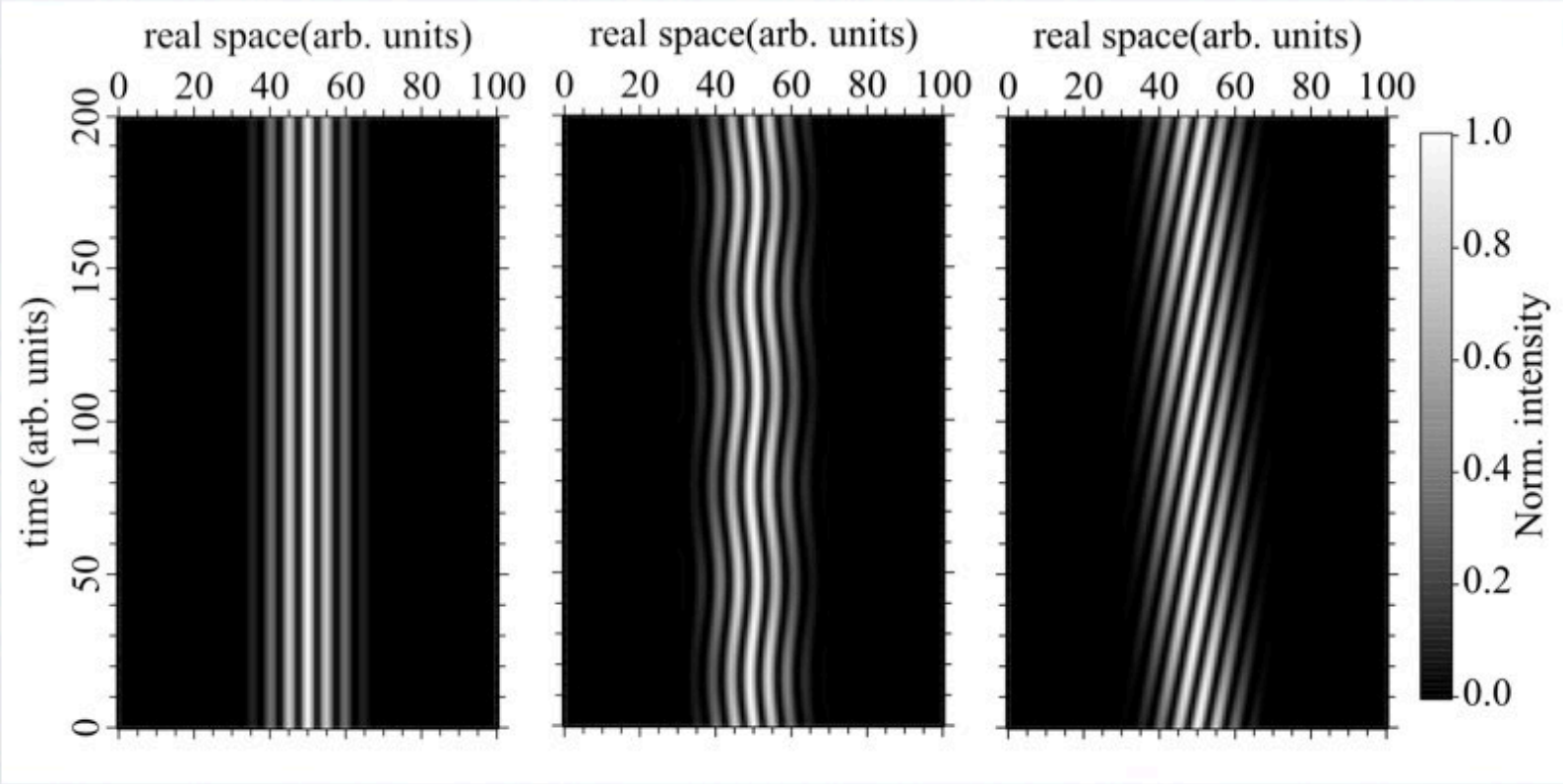

simulations : K. G. Lagoudakis

PHASE DYNAMICS

BELOW OSCILLATION THRESHOLD

ABOVE OSCILLATION THRESHOLD

CONSTANT PHASE IN TIME

LINEAR INCREASE OF THE PHASE

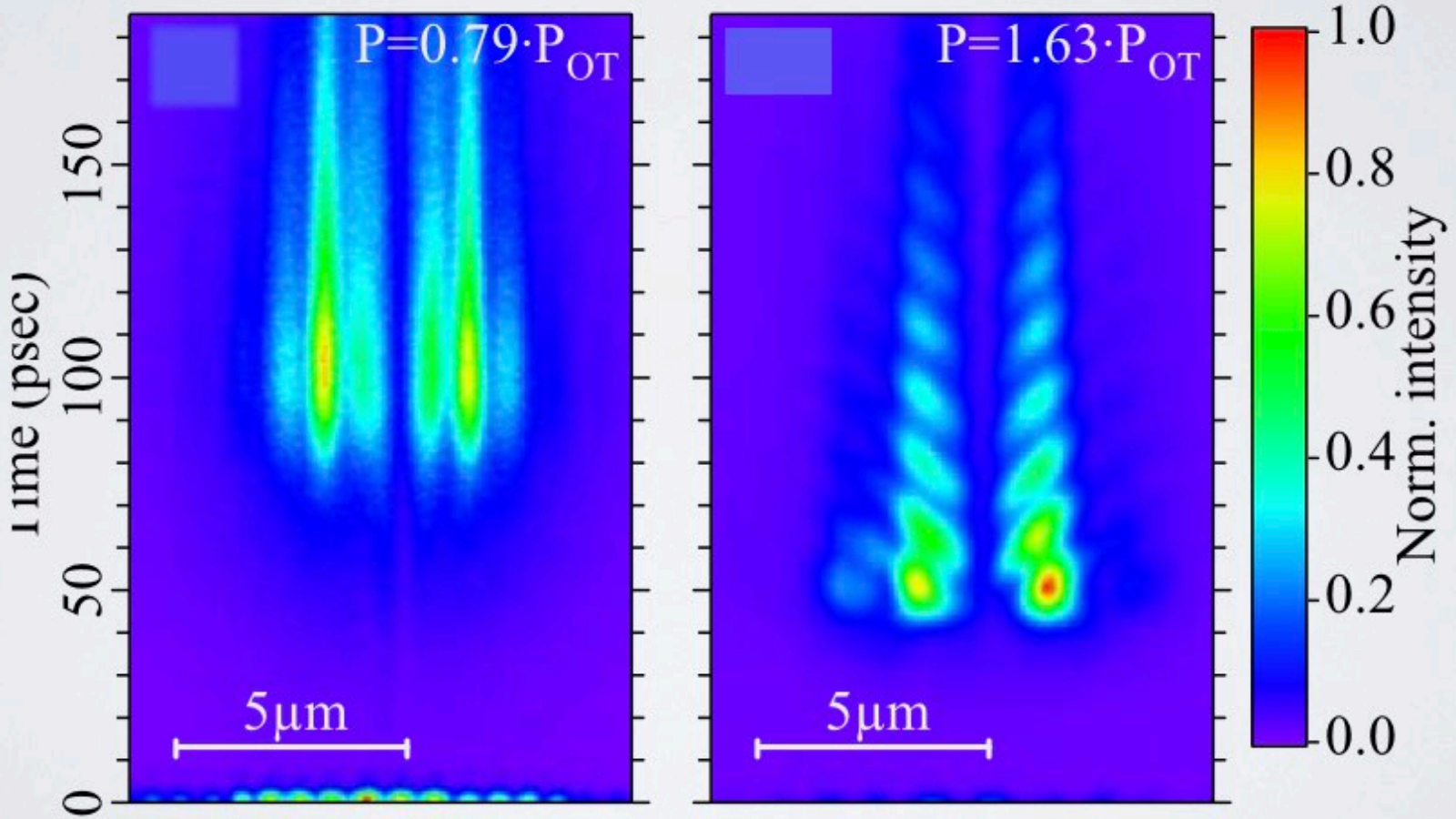

K. Lagoudakis et al., Phys. Rev. Lett. 105, 120403 (2010)

MAP OF PHASE DYNAMICS

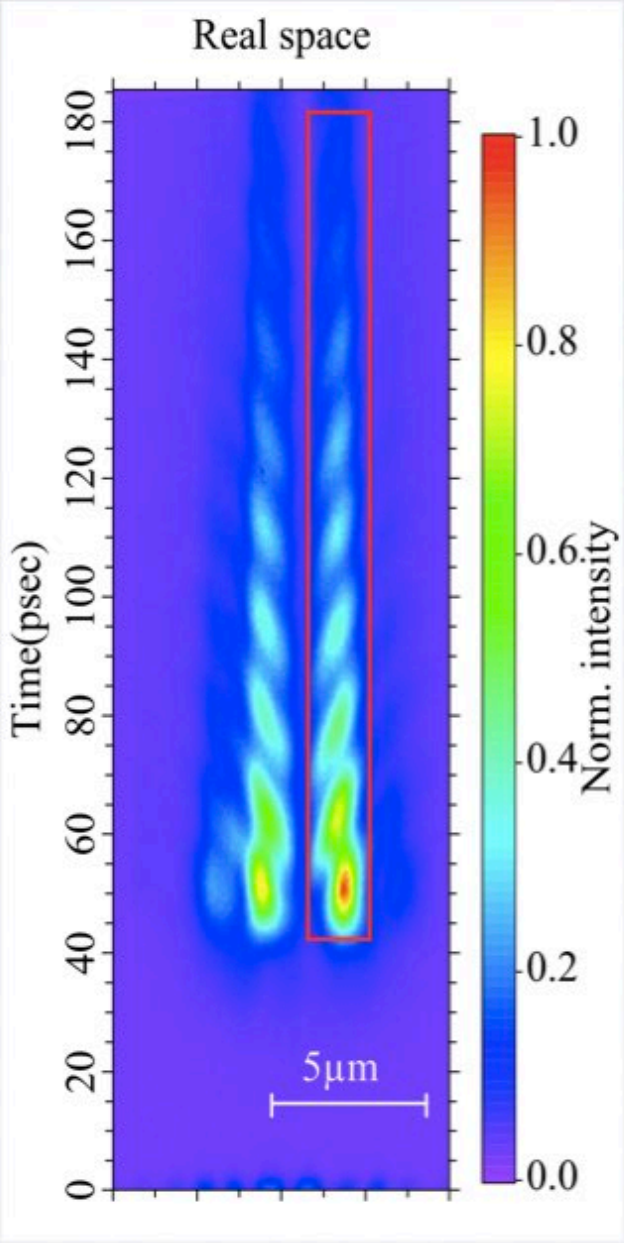

Interferogram

- Acquire interferogram for subsequent delays over 6π
- By fitting the sinusoidal behaviour in each pixel get initial phase

K. Lagoudakis et al., Phys. Rev. Lett. 105, 120403 (2010)

MAP OF PHASE DYNAMICS

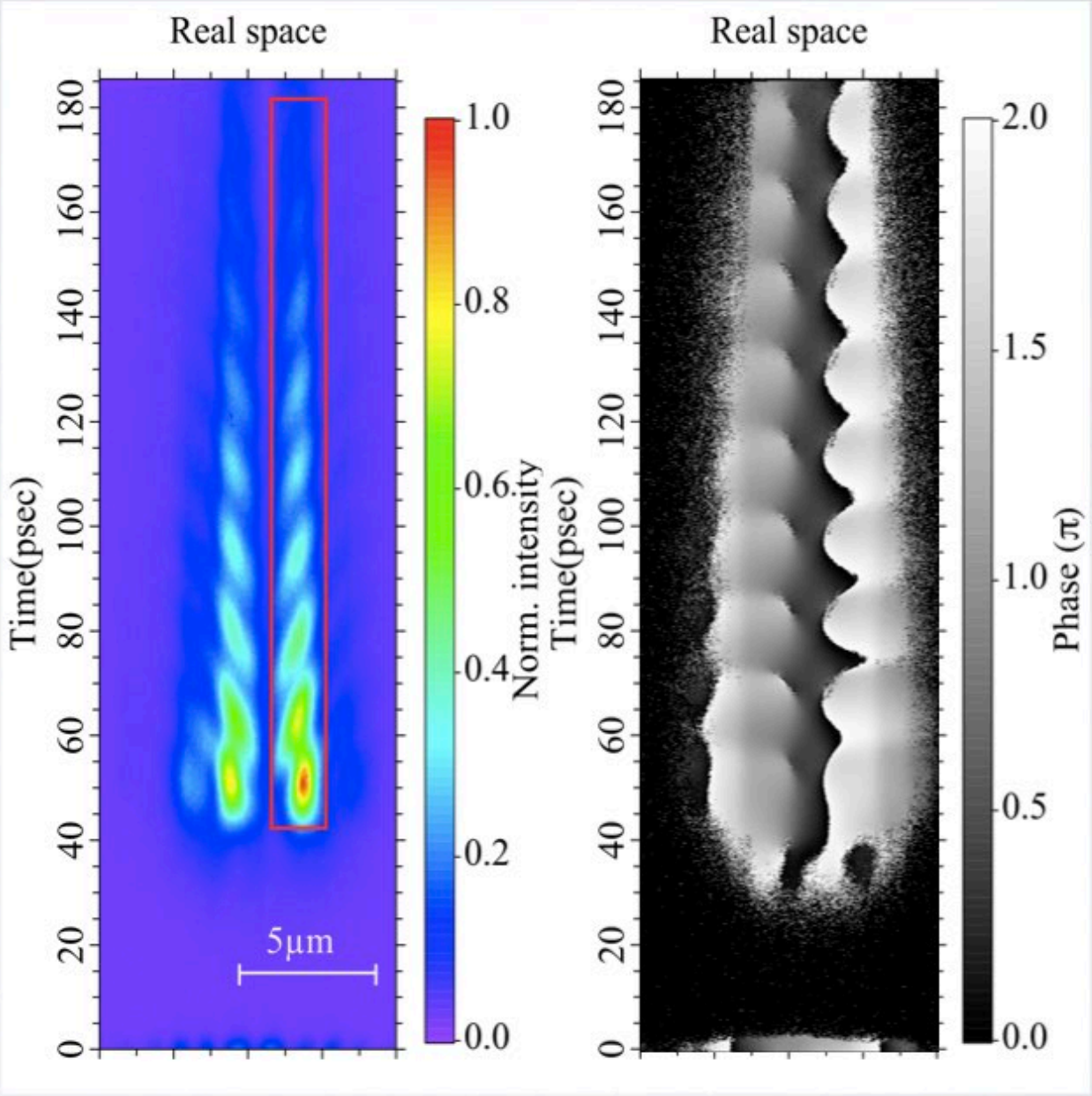

- Acquire interferogram for subsequent delays over 6π
- By fitting the sinusoidal behaviour in each pixel get initial phase

Interferogram *Phase map*

K. Lagoudakis et al., Phys. Rev. Lett. 105, 120403 (2010)

Phase oscillations

- Survive up to decay of the population
- Sawtooth (!) shape
- Linear phase evolution (modulo 2π)

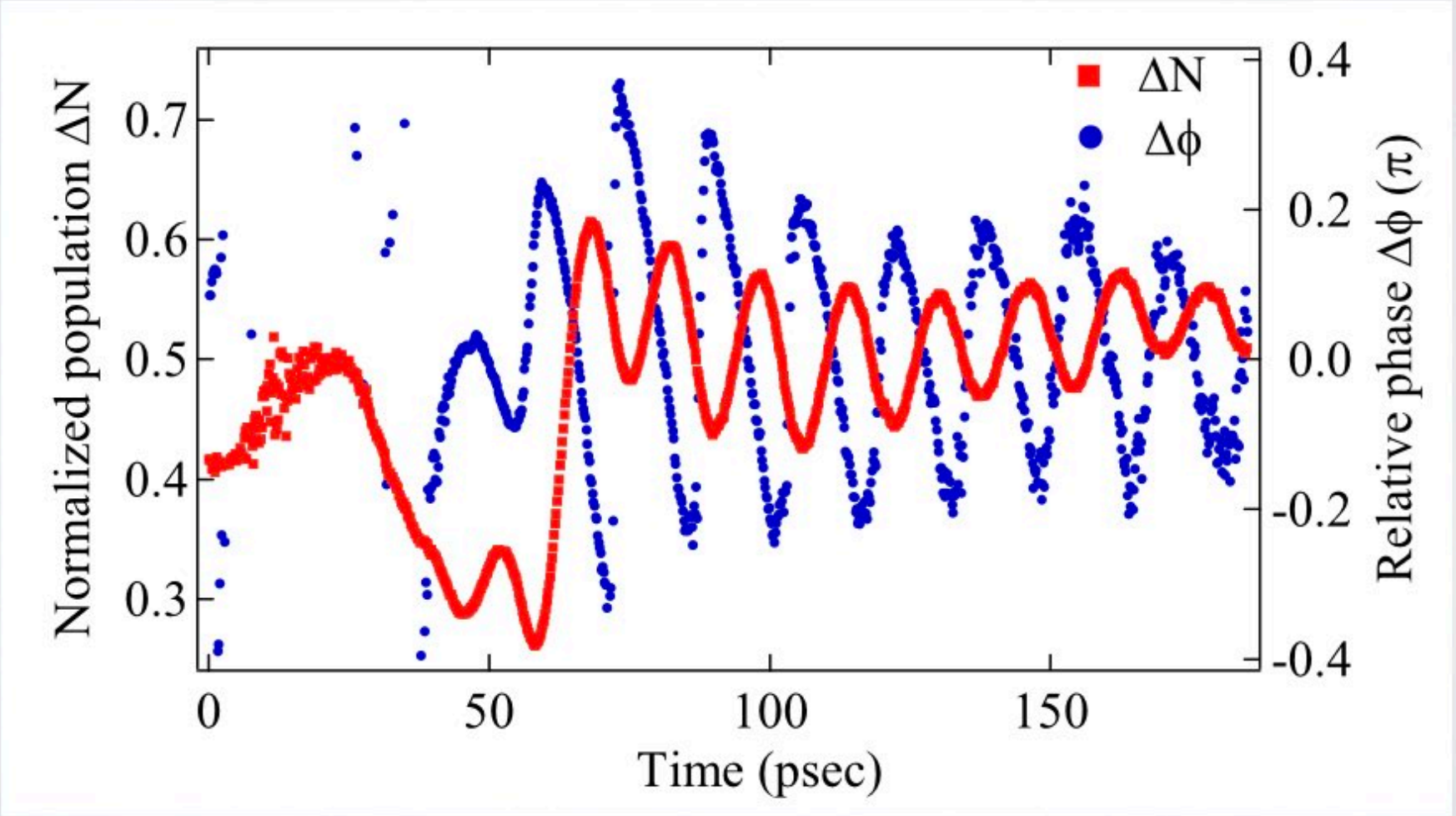

K. Lagoudakis et al., Phys. Rev. Lett. 105, 120403 (2010)

PLASMA oscillations	AC JOSEPHSON EFFECT
INITIAL CONDITION $i\hbar\frac{d\psi_L}{dt} = (E_L^0 + U|\psi_L|^2)\psi_L - J\psi_R$ $i\hbar\frac{d\psi_R}{dt} = (E_R^0 + U|\psi_R|^2)\psi_R - J\psi_L$	
no polariton - polariton interaction constant	polariton - polariton interaction energy is greater than coupling energy J
PHASE OSCILLATIONS	
sinusoidal $\hbar\omega = \sqrt{4J^2 + (E_L^0 - E_R^0)^2}$  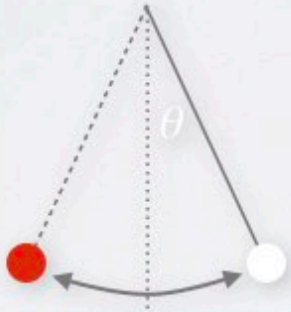	linear 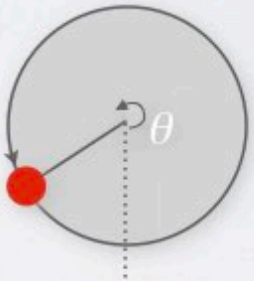  
POPULATION OSCILLATION	
damped M. Wouters and I. Carusotto, PRL 99, 140402 (2007) 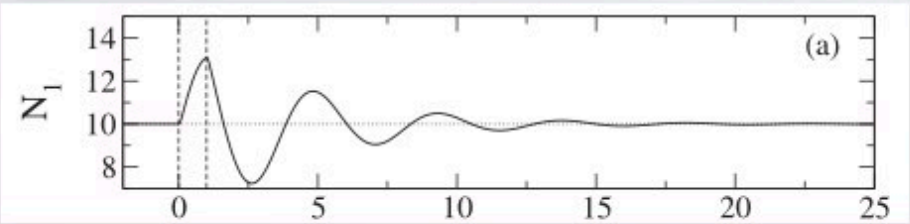	persistent 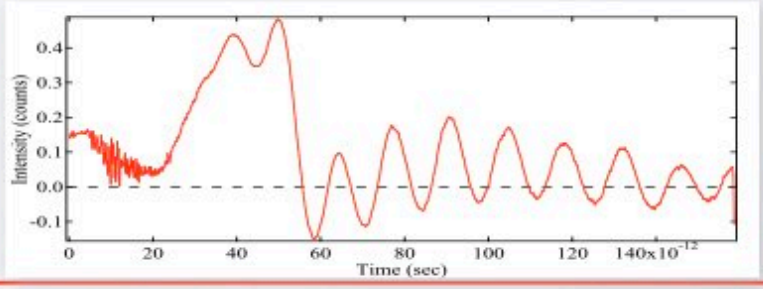

Josephson Oscillations

two coupled polariton condensates interacting by small potential barrier

M. Abbarchi, Nature Physics 9, 275 (2013)

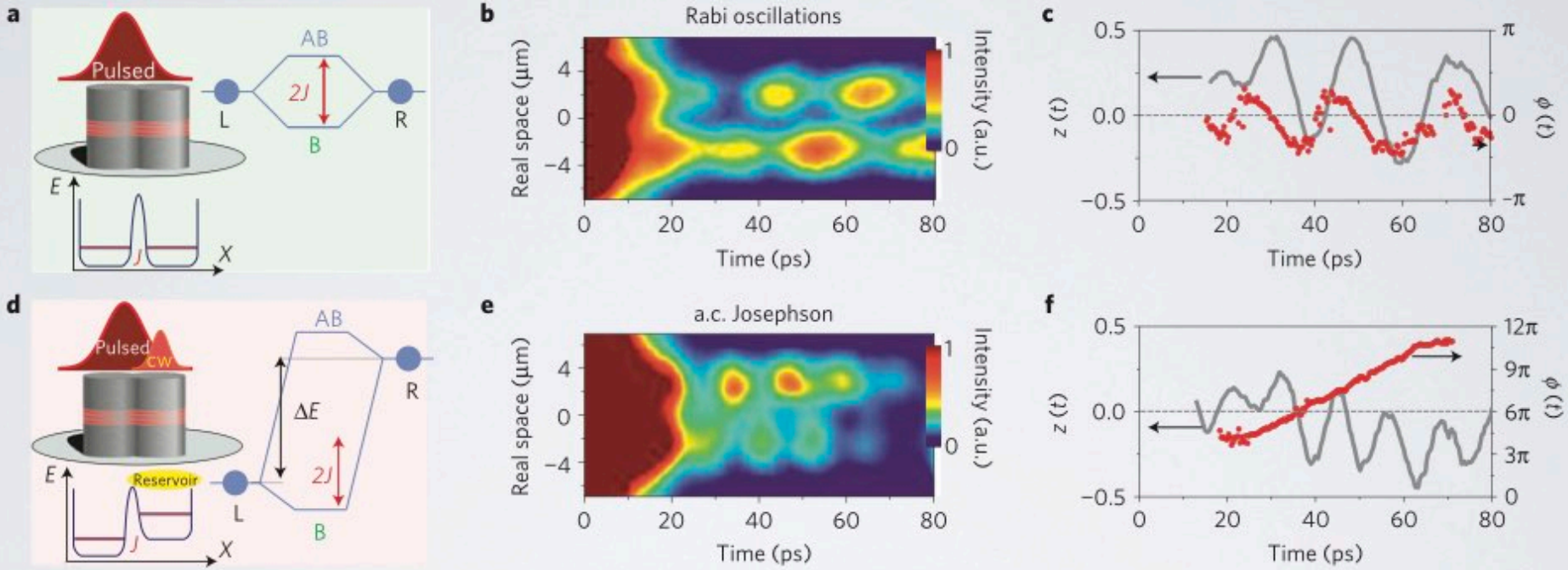

Figure 1 | Rabi oscillations and a.c. Josephson effect. a, A polaritonic molecule. The coupling J (0.1 meV) between the lowest energy state (ground state) of each micropillar (L, R) gives rise to bonding (B) and antibonding (AB) modes. **b**, Emitted intensity when an off-centred Gaussian pulse at low power (2.5 mW) excites the system. **c**, Measured population imbalance (grey line) and phase difference (red dots), showing harmonic oscillations with a frequency given by $\hbar\omega = 2J$. The slight asymmetry of the oscillations about $z = 0$ might be caused by an unintentional difference in the size of the micropillars. **d**, The a.c. Josephson regime is achieved by adding a cw beam on top of the right micropillar, which creates a reservoir (shown in yellow) inducing a static blueshift of its ground state energy. **e**–**f**, The larger bonding-antibonding splitting results in faster intensity oscillations (**e**), and in a monotonously increasing phase difference (**f**, red points).

Macroscopic quantum self-trapping

If interactions are strong enough, the self induced energy renormalization quenches the tunelling and most of the particles remian localized in one of the sites - out of equilibrium metastable regime

$$U|\psi|^2 \gg J$$

M. Abbarchi, Nature Physics 9, 275 (2013)

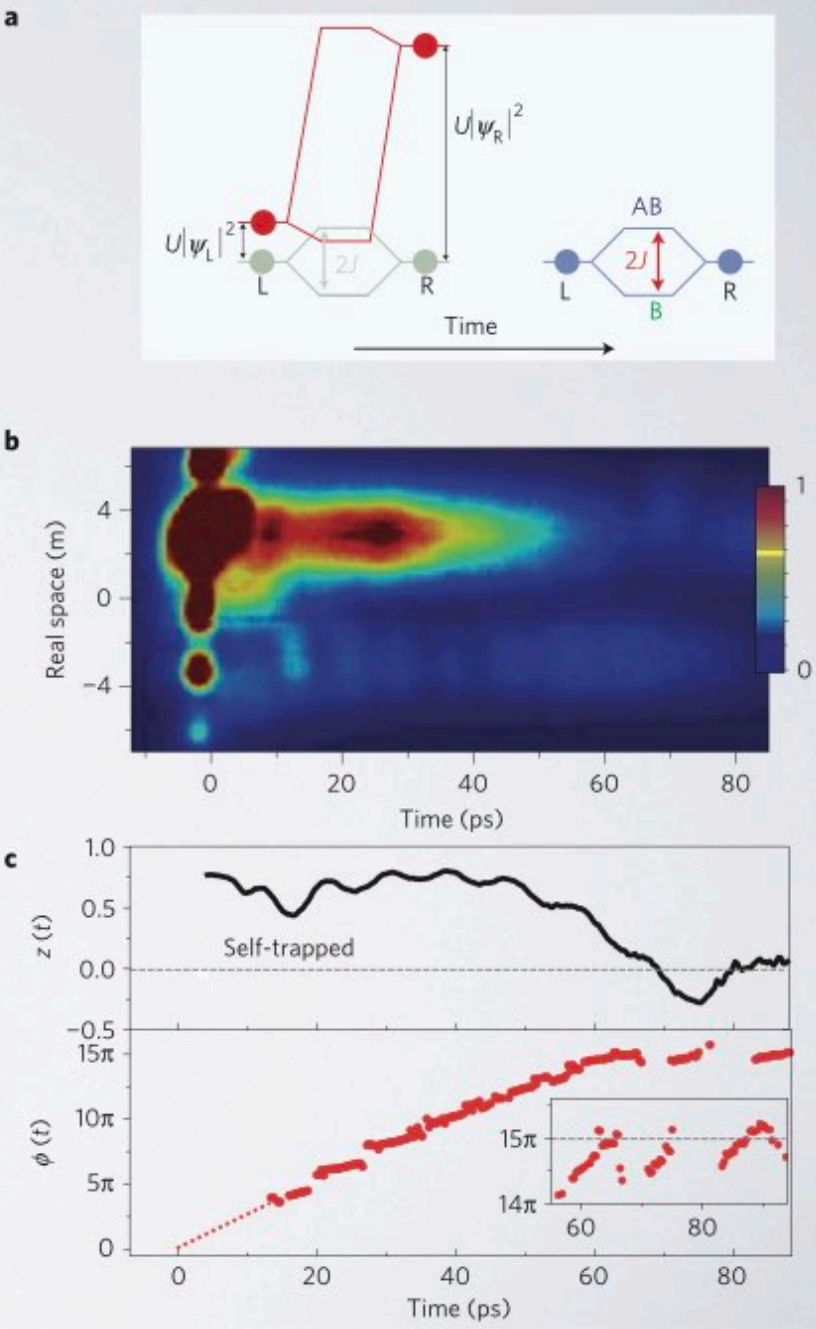

Figure 3 | Macroscopic self-trapping. a, Scheme of the renormalized energy levels at short-time (self-trapped) and long-time (harmonic oscillations) delays for a highly asymmetric excitation at high density. **b**, Measured dynamics of the emitted intensity. **c**, Time evolution of the population imbalance and phase difference. At short times particles are self-trapped in the right micropillar, and the phase difference $\phi(t)$ increases linearly with time. At $t \sim 60$ ps, the escape of particles out of the microcavity induces a transition to an oscillating regime around $\phi = 15\pi$. The red dotted line is an extrapolation of the phase evolution towards $t = 0$. **d**, Energy difference between the ground state of each micropillar extracted from the energy-resolved dynamics (see Suplementary Material). Error bars show the spectral resolution of the experiment. The energy difference is induced by the asymmetric polariton density. The transition from self-trapping to oscillations takes place when $E_R^* - E_L^* \sim 2J$.

Short summary

- Oscillating Josephson current in a polariton junction
- Relative phase increases linearly across the junction
- Fast increase rate and population asymmetry is necessary for the synchronized solution to exists

Ballistic motion

- The only force of significance is gravity
- No horizontal force is needed to maintain the horizontal motion

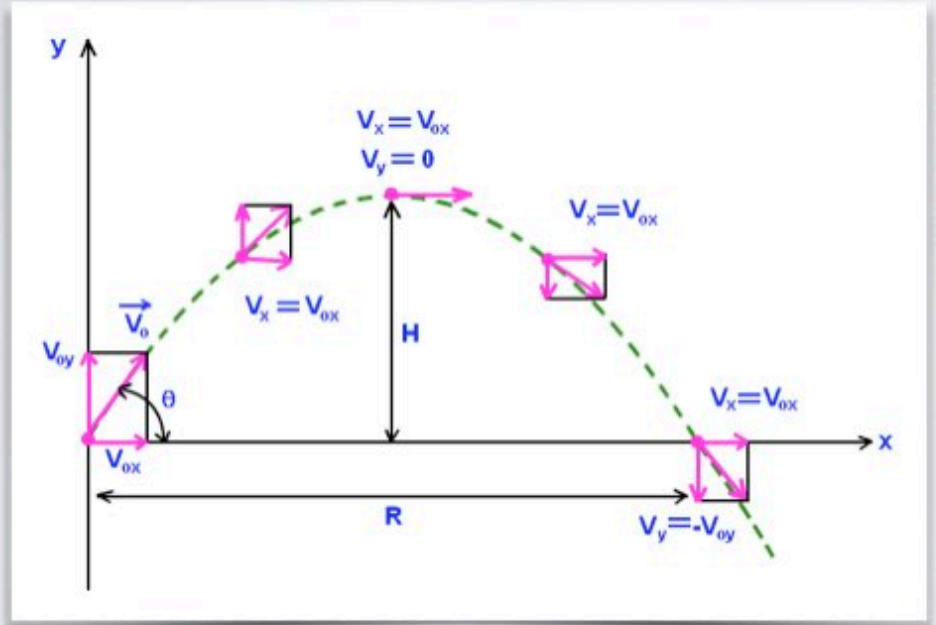

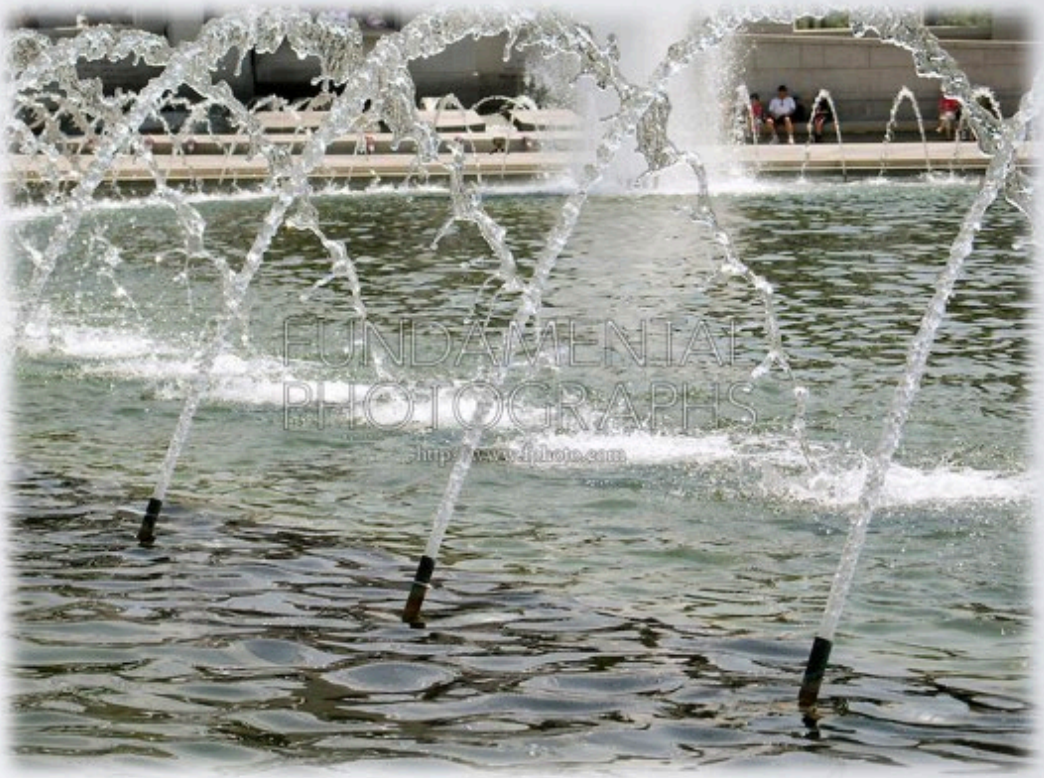

Ballistic motion

slow reflection of light

- Polariton lifetime up to 200 ps
- Microcavity quality factor 32 000

$$Q = \frac{f_0}{\Delta f} = \frac{\omega_0}{\Delta\omega}$$

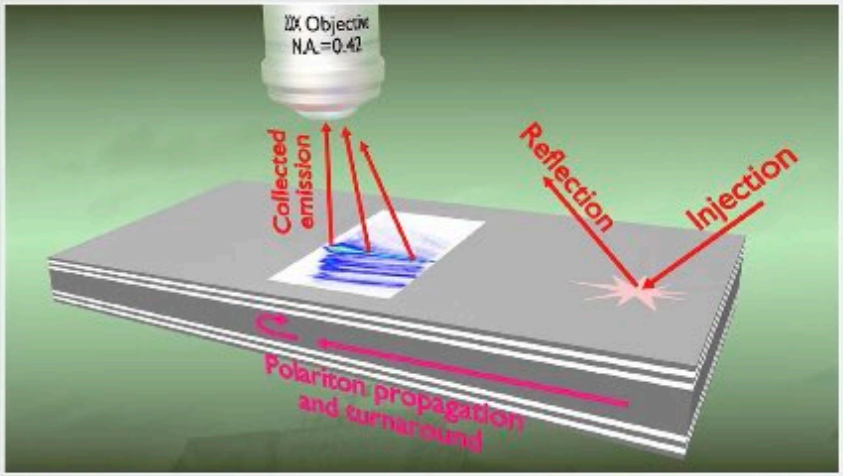

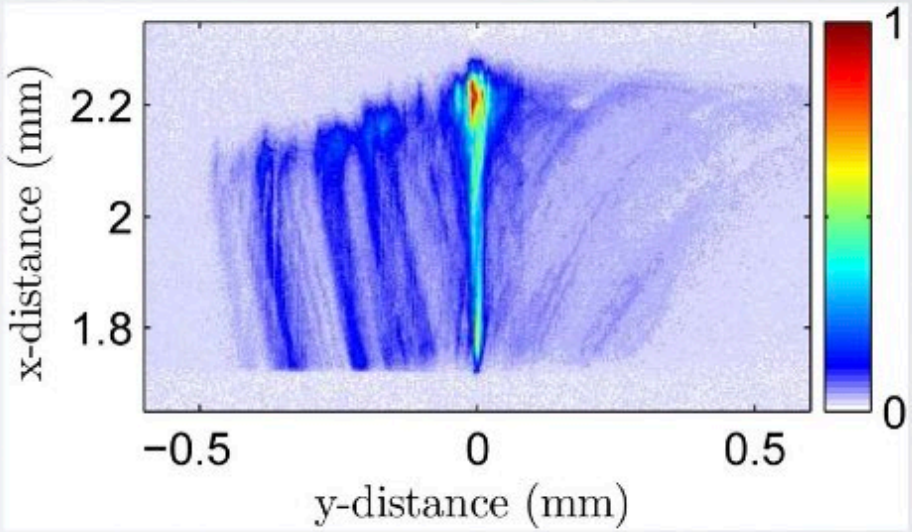

Fig. 2. Time-integrated observation of the passing polariton pulse. Coordinates are such that the point of injection is defined at $(x, y) = (0, 0)$, and the gradient is approximately toward $-x$. Polaritons approach this field of view from the left and turn around at $x \approx 2.2$ mm before flowing back to $-x$. The sharp cutoff at $x = 1.7$ mm is due to clipping in the spectrometer.

Ballistic motion

slow reflection of light

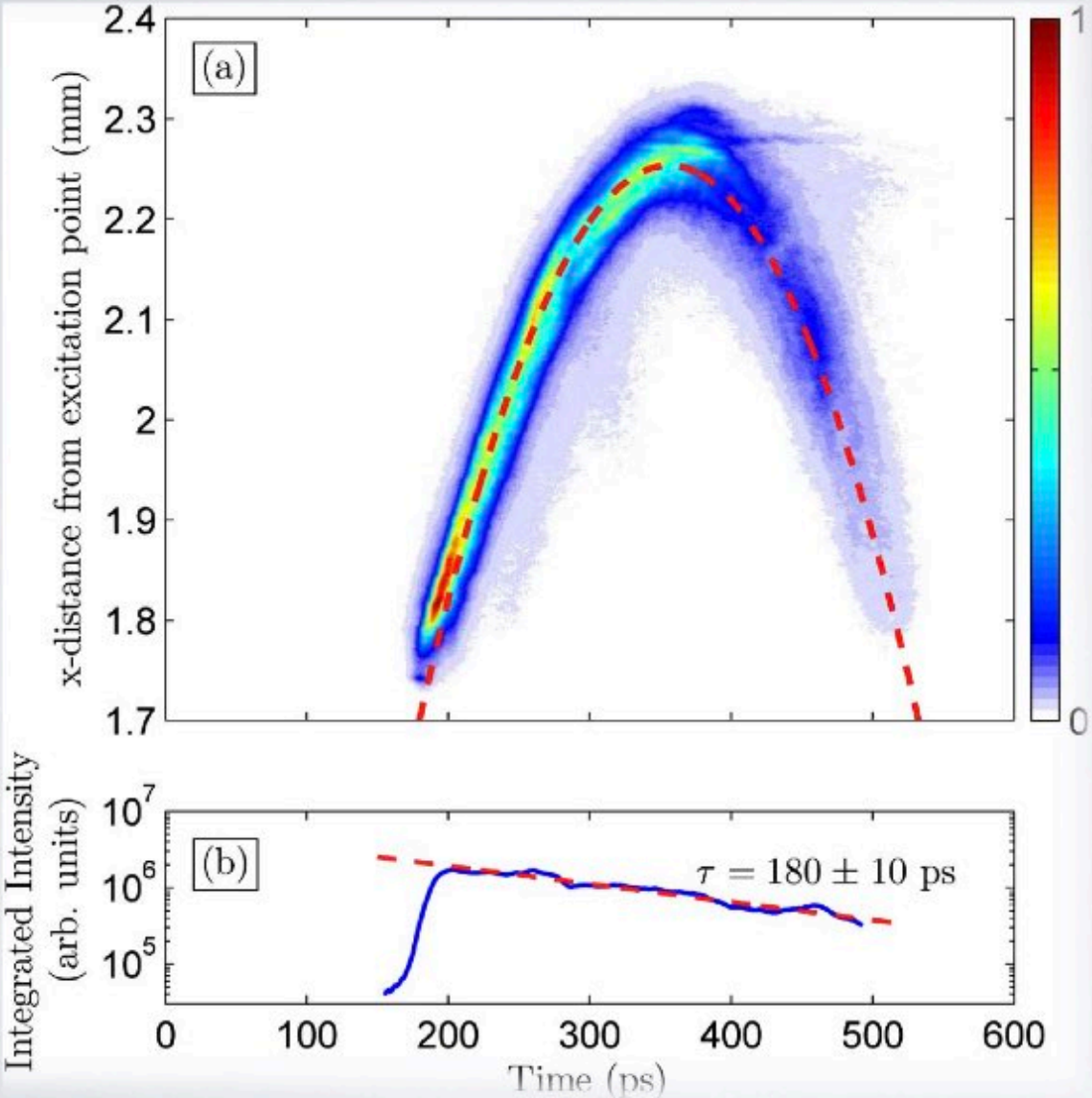

Fig. 3. Time-resolved observation of passing polariton pulses in the region of $-150\ \mu m \leq y \leq 150\ \mu m$ of Fig. 2. (a) Intensity versus x-distance versus time of the propagating polaritons. The dashed red line is a fit to the polariton motion as they feel a constant acceleration of 36 mm/ns^2. This acceleration is in good agreement with the expected value based on the known cavity gradient and the effective mass. (b) The polariton intensity of (a) summed in the x-dimension to highlight the exponential decay of the population. The data are well fit by a single exponential decay with lifetime of 180 ± 10 ps.

Polariton condensate transistor switch

PHYSICAL REVIEW B **85**, 235102 (2012)

Polariton condensate transistor switch

T. Gao,[1,2] P. S. Eldridge,[2,*] T. C. H. Liew,[3] S. I. Tsintzos,[2,4] G. Stavrinidis,[2] G. Deligeorgis,[5] Z. Hatzopoulos,[2,6] and P. G. Savvidis[1,2]

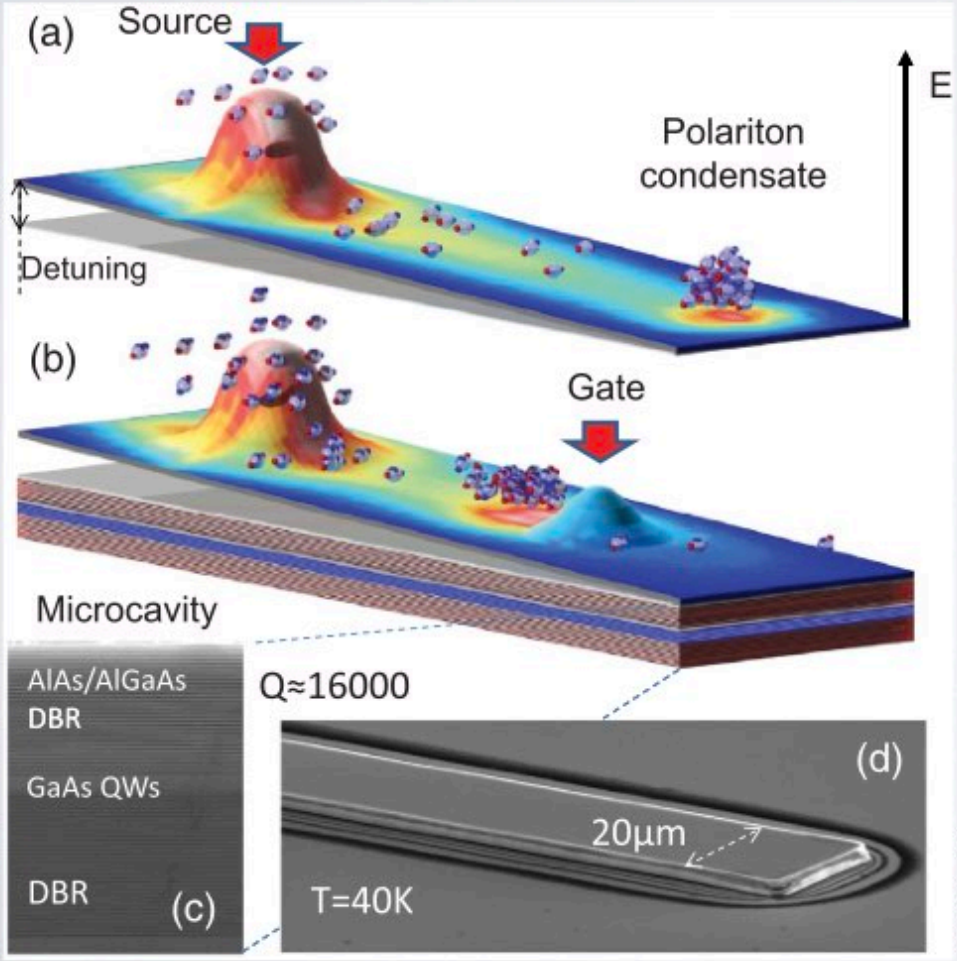

FIG. 1. (Color online) Schematic of the polariton condensate transistor based on a microcavity ridge (a) without and (b) with the gate. Scanning electron microscopy images (c) the cross section of bulk sample and (d) a 20-μm ridge.

Polariton condensate transistor switch

PHYSICAL REVIEW B **85**, 235102 (2012)

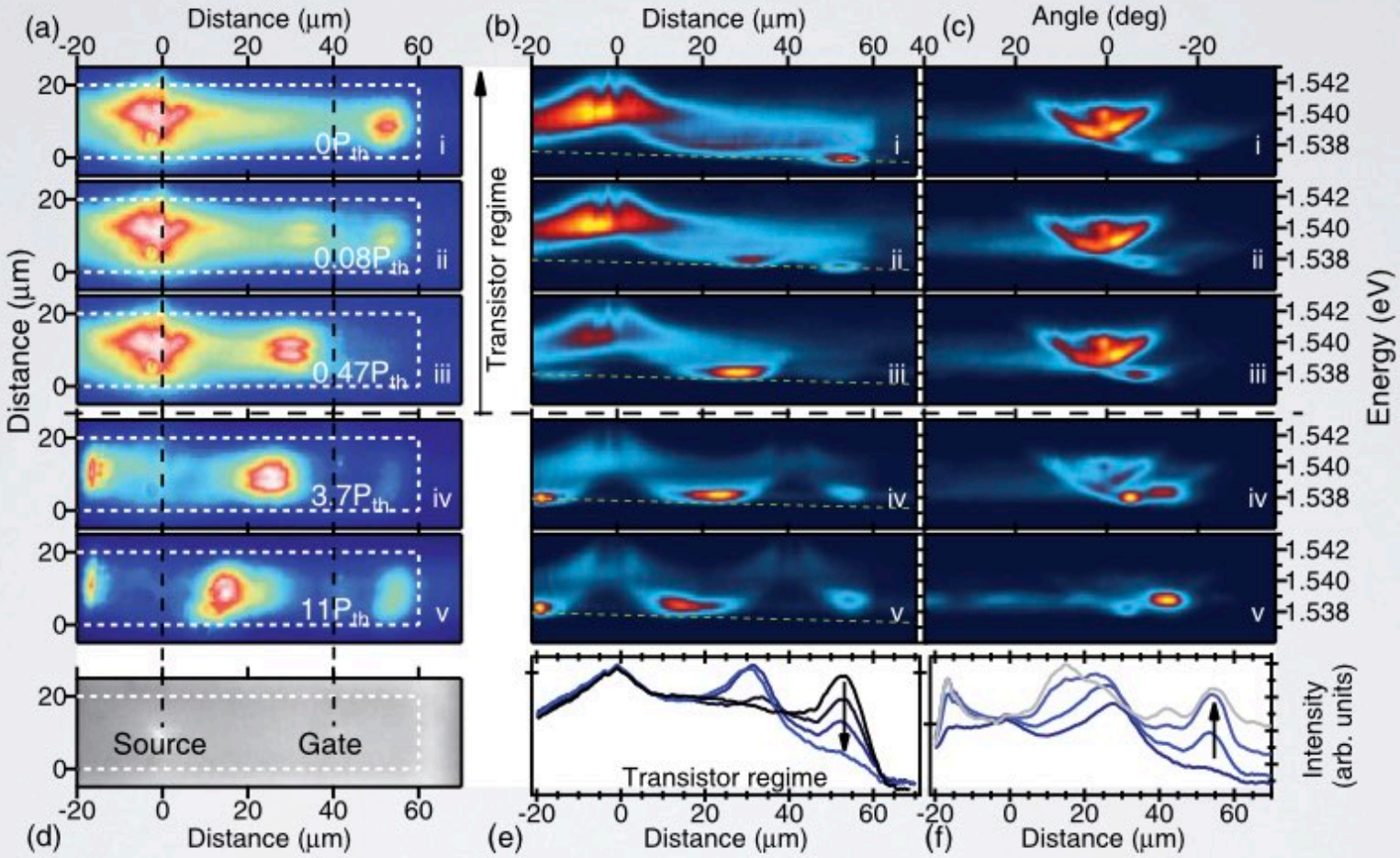

FIG. 3. (Color online) (a) Real-space, (b) energy-real space, and (c) energy-angle space images for different gate powers (i–v) for a constant source power ($10P_{th}$). (d) White light image of the ridge showing the positions of the source and the gate. The line profile (log scale) along the center of the ridge for a gate power (e) below and (f) above threshold for increasing gate power (as indicated by arrow).

Polariton condensate transistor switch

C. Anton, D. M. Martin, C. Tejedor, L. Vina, UAM, Madrid

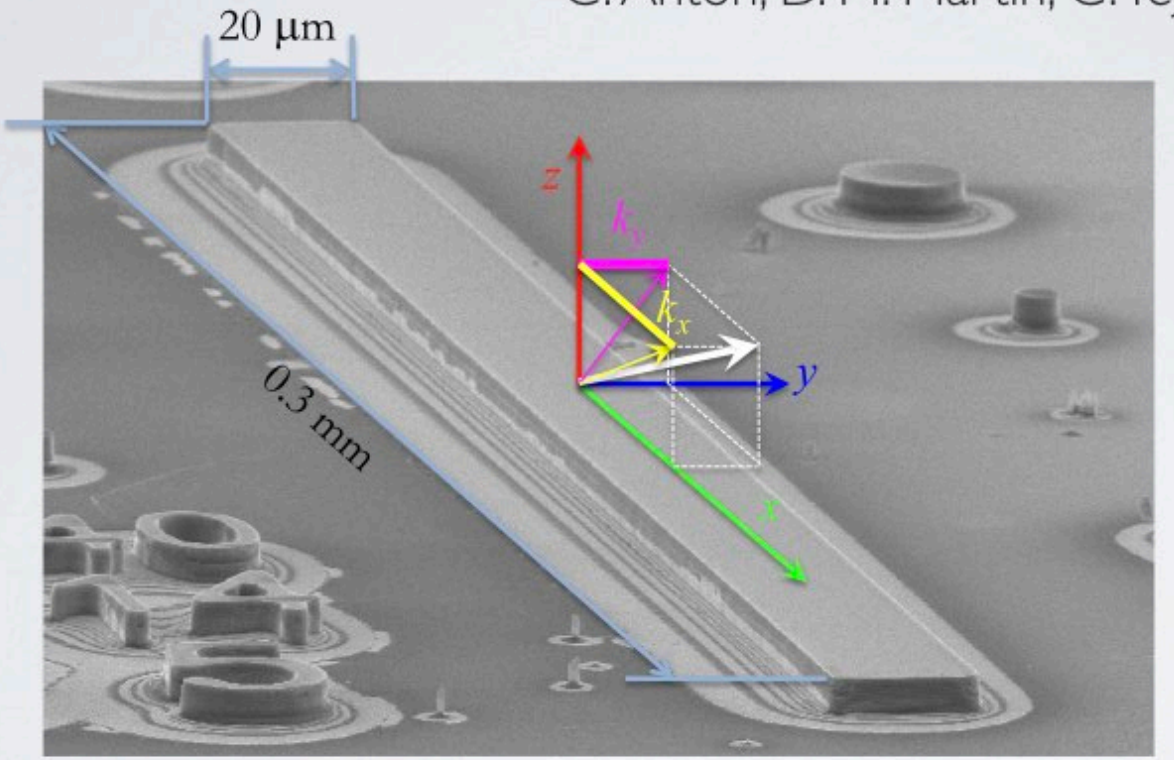

high-quality AlGaAs-based microcavity

Polariton condensate transistor switch

C. Anton, D. M. Martin, C. Tejedor, L. Vina, UAM, Madrid

Experiments on transistor switch